THE SUNYAEV-ZELDOVICH EFFECT: CURRENT STATUS AND FUTURE PROSPECTS

YOEL REPHAELI

School of Physics & Astronomy, Tel Aviv University, Tel Aviv 69978, Israel
E-mail: yoelr@wise1.tau.ac.il

The detailed spectral and spatial characteristics of the signature imprinted on the cosmic microwave background (CMB) radiation by Compton scattering of the radiation by electrons in the hot gas in clusters of galaxies - the Sunyaev-Zeldovich (S-Z) effect - are of great astrophysical and cosmological significance. In recent years observations of the effect have improved tremendously; high signal-to-noise images of the effect (at low microwave frequencies) can now be obtained by interferometric arrays. In the near future, high frequency measurements of the effect will be made with ground based and balloon-borne telescopes equipped with bolometeric arrays. Towards the end of the decade the PLANCK satellite will carry out an extensive S-Z survey over a wide frequency range. Along with the improved observational capabilities, the theoretical description of the effect, and its use as a precise cosmological probe, have been considerably advanced. In this review, I briefly discuss the nature and significance of the effect, its exact theoretical description, the current observational status, and prospects for the near future.

1   Introduction

The S-Z effect was first described by Zeldovich & Sunyaev (1969) and Sunyaev & Zeldovich (1972), and after many attempts over a decade, it was convincingly detected in several clusters by single-dish radio telescopes (for general reviews, see Rephaeli 1995a, Birkinshaw 1999). Increased realization of the cosmological significance of the effect has led to major improvements in observational techniques and to extensive theoretical investigations of many of its facets. The most important recent development is the ability to carry out sensitive radio interferometric measurements of the effect (Jones 1993, Carlstrom *et al.* 1996). Impressive images of the effect in more than thirty clusters have already been obtained using the OVRO and BIMA arrays (Carlstrom *et al.* 1999, Carlstrom *et al.* 2000). Theoretical treatment of the S-Z effect has also improved, starting with the work of Rephaeli (1995b), who performed an exact relativistic calculation and demonstrated the need for such a more accurate description.

The effect is a direct probe of clusters; high resolution measurements yield the spatial distributions of the hot intracluster (IC) gas and the *total* mass, as well as information on the evolution of clusters. Of more basic importance is the ability to determine the Hubble constant, H_0, and the density parameter, Ω, from S-Z and X-ray measurements. This method to determine H_0, which has clear advantages over the traditional galactic distance ladder method, has already been employed but its full potential has not yet been realized because of substantial observational uncertainties. Sensitive mapping of the effect, and the understanding and minimization of systematic uncertainties in the S-Z and X-ray measurements, are essential steps towards this goal and constitute the main challenge of current and near future work on the S-Z effect.

The recent progress in S-Z work, and especially the improved spectral and spatial capabilities that will be attained in the near future by ground based and stratospheric projects, will advance this field to the forefront of cosmological research. Here I review recent progress in this field and briefly discuss the prospects for the near future.

2   Exact Description of the Effect

Compton scattering of the CMB by hot gas heats the radiation, resulting in a systematic transfer of photons from the Rayleigh-Jeans (R-J) to the Wien side of the (Planckian) spectrum. An accurate description of the interaction of the radiation with a hot electron gas necessitates the calculation of the exact frequency re-distribution function in the context of a relativistic formulation. The calculations of Sunyaev & Zeldovich (1972) are based on a solution to the *nonrelativistic* Kompaneets (1957) equation. The result of their treatment is a simple expression for the intensity change resulting from the scattering off electrons with thermal velocity distribution, ΔI_t, in terms of the Comptonization parameter, $y = \int (kT_e/mc^2)n\sigma_T dl$. This is a line of sight integral (through the cluster) over the electron density (n) and temperature (T_e); σ_T is the Thomson cross section. ΔI_t is negative in the R-J region and positive at frequencies above a critical value ~ 217 GHz ($x \equiv h\nu/kT = 3.83$). Typically, in a rich cluster, $y \sim 10^{-4}$, along a line of sight through the center, and the magnitude of the relative temperature change due to the thermal effect is $\Delta T_t/T_0 = -2y \sim -2 \cdot 10^{-4}$ in the R-J region.

The effect has a second component when the cluster has a finite (peculiar) velocity in the CMB frame. This kinematic Doppler component, which is obviously proportional to the component of the cluster peculiar velocity along the line of sight, v_r, and to the Thomson optical depth, is $\Delta I_k = x^4 e^x (v_r/c)\tau/(e^x - 1)^2$. The related temperature change is $\Delta T_k/T_0 = -(v_r/c)\tau$ (Sunyaev & Zeldovich 1980).

The nonrelativistic treatment of Sunyaev & Zeldovich (1972) is generally valid at low gas temperatures and at low frequencies. Rephaeli (1995b) has shown that this approximation is insufficiently accurate for use of the effect as a precise cosmological probe: Electron velocities in the IC gas are high, and the relative photon energy change in the scattering is appreciable enough to require a relativistic calculation. Using the exact probability distribution in Compton scattering, and the relativistically correct form of the electron Maxwellian velocity distribution, Rephaeli (1995b) calculated ΔI_t in the limit of small τ, keeping terms linear in τ (single scattering). Results of this semi-analytic calculation, shown in Figure 1, demonstrate that the relativistic spectral distribution of the intensity change is quite different from that derived by Sunyaev & Zeldovich (1972). Deviations from their expression increase with T_e and can be quite substantial. These are especially large near the crossover frequency (where ΔT_t changes sign) which shifts to higher values with increasing gas temperature.

The work of Rephaeli (1995b) sparked considerable interest which led to various generalizations and extensions of the relativistic treatment of the S-Z effect. Challinor & Lasenby (1998) generalized the Kompaneets equation and obtained analytic approximations to its solution for the change of the photon occupation
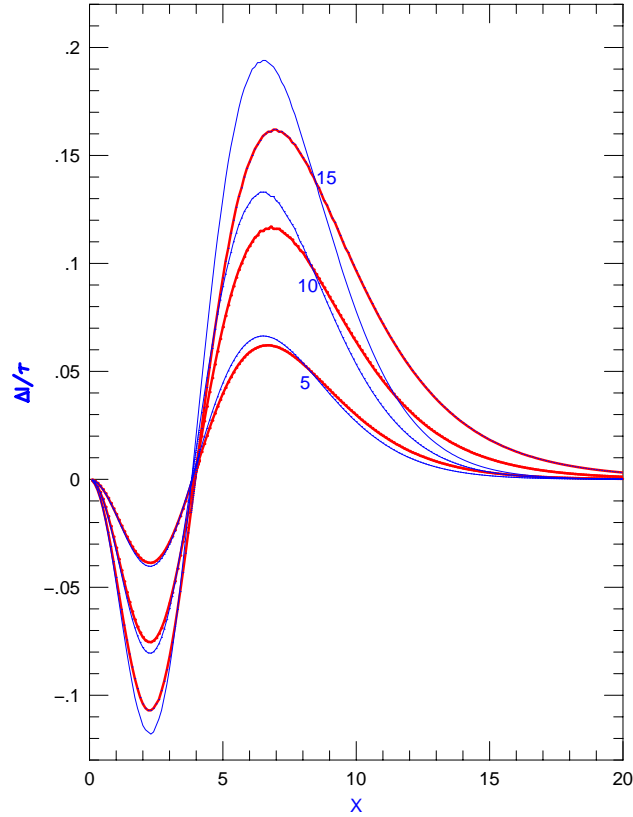
Figure 1. The spectral distribution of $\Delta I_t/\tau$ [in units of $(hc)^2/(2(kT_o)^3)$]. The pairs of thick (red) and thin (blue) lines show the relativistic and nonrelativistic distributions, respectively. Three pairs of lines are shown corresponding to $kT_e = 5$, 10, and 15 keV.

number by means of a power series in $\theta_e = kT_e/mc^2$. Itoh *et al.* (1998) adopted this approach and improved the accuracy of the analytic approximation by expanding to fifth order in θ_e. Sazonov & Sunyaev (1998) and Nozawa *et al.* (1998) have extended the relativistic treatment also to the kinematic component obtaining – for the first time – the leading cross terms in the expression for the total intensity change ($\Delta I = \Delta I_t + \Delta I_k$) which depend on both T_e and v_r. An improved analytic fit to the results of numerical integration (of the collision term in the Boltzmann equation), valid for $0.02 \leq \theta_e \leq 0.05$, and $x \leq 20$ ($\nu \leq 1130$ GHz), has recently been given by Nozawa *et al.* (2000). In view of the possibility that in some rich clusters $\tau \sim 0.02 - 0.03$, the approximate analytic expansion to fifth order in θ_e necessitates self-consistent inclusion also of multiple scatterings, of order τ^2. This has been accomplished by Itoh *et al.* (2000), and Shimon & Rephaeli (2001).

The relativistically correct calculation has to be used in all high frequency S-Z

work, especially when measurements of the effect are used to determine precise values of the cosmological parameters. Also, since the ability to determine peculiar velocities of clusters depends very much on measurements at or very near the crossover frequency, its exact value has to be known. This necessitates knowledge of the gas temperature since in the exact relativistic treatment the crossover frequency is no longer independent of the gas temperature, and is approximately given by $\simeq 217[1 + 1.167kT_e/mc^2 - 0.853(kT_e/mc^2)^2]$ GHz (Nozawa et $al.$ 1998a).

Use of the S-Z effect as a cosmological probe necessitates also X-ray measurements to determine (at least) the gas temperature. Therefore, a relativistically correct expression for the (spectral) bremsstrahlung emissivity must be used (Rephaeli & Yankovitch 1997). In the latter paper first order relativistic corrections to the velocity distribution, and electron-electron bremsstrahlung, were taken into account in correcting values of H_0 that were previously derived using the nonrelativistic expression for the emissivity (see also Hughes & Birkinshaw 1998). Nozawa et $al.$ (1998b) have performed a more exact calculation of the relativistic bremsstrahlung Gaunt factor.

Compton scattering of the CMB in clusters also affects its polarization towards the cluster. Net polarization is induced due to the quadrupole component in the spatial distribution of the radiation, and when the cluster peculiar velocity has a component transverse to the line of sight, $v_\perp$ (Sunyaev & Zeldovich 1980, Sazonov & Sunyaev 1999). The leading contributions to the latter, kinematically-induced polarization, are proportional to $(v_\perp/c)\tau^2$ and $(v_\perp/c)^2\tau$. Itoh et $al.$ (2000) have included relativistic corrections in the expression for the kinematic polarization.

3   Recent Measurements

The dramatic improvements in the quality of S-Z measurements over the last seven years is largely due to the use of interferometric arrays. Dish arrays have several major advantages over a single dish, including insensitivity to changes in the atmospheric emission, sensitivity to specific angular scales and to signals which are correlated between the array elements, and the high angular resolution that enables nearly optimal subtraction of signals from point sources. With the improved sensitivity of radio receivers it became advantageous to use interferometric arrays for S-Z imaging measurements (starting with the use of the Ryle telescope by Jones et $al.$ 1993). Current state-of-the-art work is done with the BIMA and OVRO arrays; images of some 35 moderately distant clusters (in the redshift range $0.17 - 0.89$) have already been obtained at ~ 30 GHz (Carlstrom et $al.$ 1999, 2000). A beautiful example is the 28 GHz image of the cluster CL0016+16 obtained with the BIMA array (Carlstrom et $al.$ 1999) which is shown in Figure 2. The ROSAT X-ray image is superposed on the contour lines of the S-Z profile in the lower frame; note the good agreement between the orientation of the X-ray and S-Z brightness distributions.

Work has begun recently with the CBI, a new radio (26-36 GHz) interferometric array (in the Chilean Andes) of small (0.9m) dishes on a platform with baselines in the 1m to 6m range. The spatial resolution of the CBI is in the $3' - 10'$ range, so (unlike the BIMA and OVRO arrays) it is suitable for S-Z measurements of nearby clusters. Some 9 clusters have already been observed with the CBI (Udomprasert
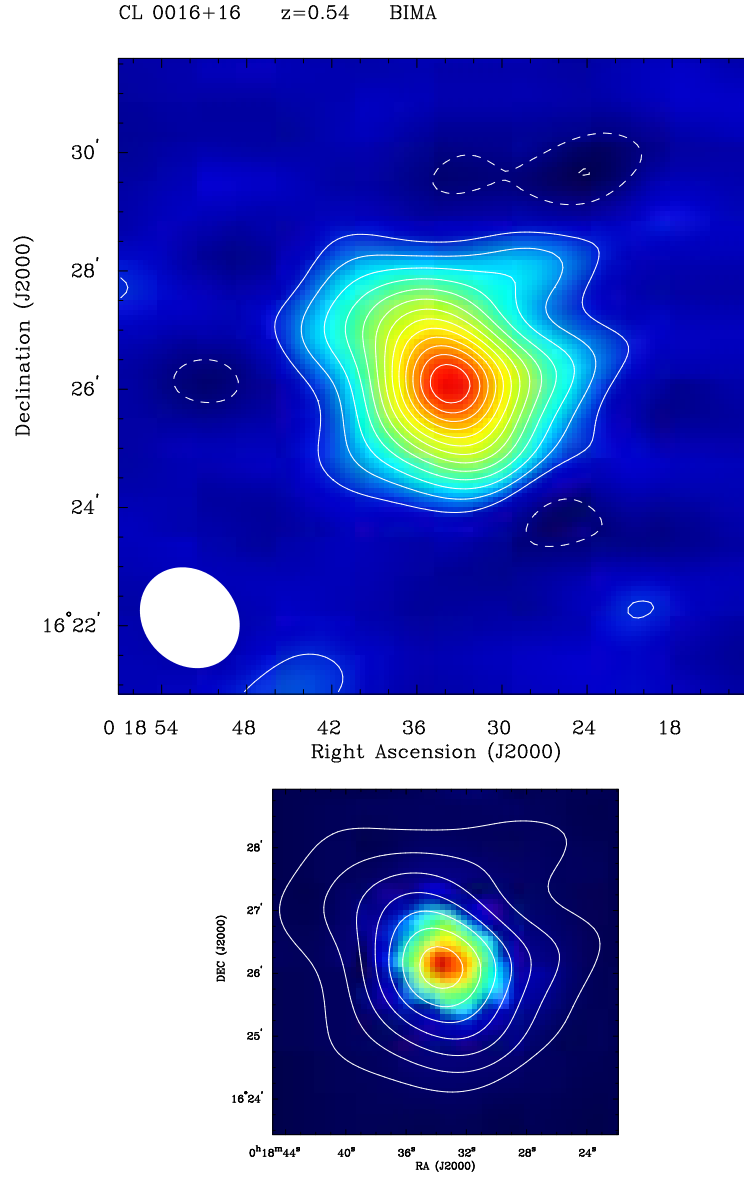
CL 0016+16   z=0.54   BIMA

Figure 2. S-Z and X-ray images of the cluster CL0016+16. The S-Z image (false color) of the cluster, obtained with the BIMA array, is shown in the upper frame. In the lower frame, contours of the S-Z effect in the cluster are superposed on the *ROSAT* X-ray (false color) image (from Carlstrom *et al.* 1999).

et al. 2000).

Recent work at higher frequencies includes measurements with the SuZIE array, and the PRONAOS and MITO telescopes. SuZIE (which was previously used to measure the effect towards the moderately distant clusters A1689 & A2163 Holzapfel *et al.* 1997a, 1997b) observed the effect towards A1835 at three spectral bands centered on 145, 221, 279 GHz (Mauskopf *et al.* 2000). Observations at four wide spectral bands (in the overall range of 285-1765 GHz) were made of A2163 with the PRONAOS atmospheric 2m telescope (Lamarre *et al.* 1998), leading to what seems to be the first detection of the effect by a balloon-borne experiment. The new 2.6m MITO telescope – which currently operates at four spectral bands and has a large $\sim 17'$ beam – was used to observe the effect in the Coma cluster (Lamagna *et al.* , these proceedings). The strongest S-Z effect, with $y = 1.2 \times 10^{-3}$, seems to have been detected towards the distant (z=0.45) cluster RXJ 1347 (Pointecouteau *et al.* 1999) with the Diabolo bolometer operating at the IRAM 30m radio telescope. The Diabolo has a $0.5'$ beam, and a dual channel bolometer (centered on 2.1 and 1.2 mm). Four other clusters were also observed with diabolo (Desert *et al.* 1998).

4   The Effect as a Cosmological Probe

The S-Z effect is a unique probe whose indispensable qualities are being increasingly exploited for the determination of cluster and global cosmological parameters. For an extensive discussion of use of the effect as a probe, see the reviews by Rephaeli (1995a), and Birkinshaw (1999).

In principle, high spatial resolution measurements of the S-Z effect yield the gas temperature and density profiles across the cluster. The deduction of an approximate 3D density and temperature distributions from their sky-projected profiles requires use of a deprojection algorithm. One such was developed by Zaroubi *et al.* (1998; see also the contribution by Zaroubi to these proceedings). Cluster gas density and temperature profiles have been mostly deduced from X-ray measurements. S-Z measurements can more fully determine these profiles due to the linear dependence of ΔI_t on n, as compared to the n^2 dependence of the (thermal bremsstrahlung) X-ray brightness profile.

The cluster full mass profile, $M(r)$, can be derived directly from the gas density and temperature distributions by solving the equation of hydrostatic equilibrium (assuming, of course, the gas has reached such a state in the underlying gravitational potential). This method has already been employed in many analyses using X-ray deduced gas parameters (*e.g.,* Fabricant *et al.* 1980). Grego *et al.* (2001) have recently used this method to determine total masses and gas mass fractions of 18 clusters based largely on the results of their interferometric S-Z measurements. Isothermal gas with the familiar density profile, $(1+r^2/r_c^2)^{-3\beta/2}$, was assumed. The core radius, r_c, and β were determined from analysis of the S-Z data, whereas the X-ray value of the temperature was adopted. Mean values of the gas mass fraction were found to be in the range $(0.06 - 0.09)h^{-1}$ (where h is the value of H_0 in units of 100 km s^{-1} Mpc^{-1}) for the currently popular open and flat, Λ-dominated, CDM models.

Measurement of the kinematic S-Z effect yields the line of sight component of the cluster peculiar velocity (v_r). This is observationally feasible only in a narrow spectral band near the critical frequency, where the thermal effect vanishes while the kinematic effect – which is usually swamped by the much larger thermal component – is maximal (Rephaeli & Lahav 1991). SuZIE is the first experiment with a spectral band centered on the crossover frequency. Measurements of the clusters A1689 and A2163 (Holzapfel $et\ al.$ 1997b) and A1835 (Mauskopf $et\ al.$ 2000) yielded substantially uncertain results for v_r (170^{+815}_{-630}, 490^{+1370}_{-880}, and 500 ± 1000 km s^{-1}, respectively).

Perhaps the most important use of the S-Z effect so far has been the measurement of the Hubble constant, H_0, and the cosmological density parameter, Ω. Briefly, the method is based on determining the angular diameter distance, d_A, from a combination of ΔI_t, the X-ray surface brightness, and their spatial profiles. Averaging over the first eight determinations of H_0 (from S-Z and X-ray measurements of seven clusters) yielded $H_0 \simeq 58 \pm 6$ km s^{-1} Mpc^{-1} (Rephaeli 1995a), but the database was very non-uniform and the errors did not include systematic uncertainties. Repeating this with a somewhat updated data set, Birkinshaw (1999) deduced essentially a similar mean value. A much larger S-Z data set is now available from the interferometric BIMA and OVRO observations, and since the redshift range of the clusters in the sample is substantial, the dependence on Ω is appreciable. A fit to 33 cluster distances gives $H_0 = 60$ km s^{-1} Mpc^{-1} for $\Omega = 0.3$, and $H_0 = 58$ km s^{-1} Mpc^{-1} for $\Omega = 1$, with direct observational errors of $\pm 5\%$ (Carlstrom $et\ al.$ 2000). The main known sources of systematic uncertainties (see discussions in Rephaeli 1995a, and Birkinshaw 1999) are presumed to introduce an additional error of $\sim 30\%$ (Carlstrom $et\ al.$ 2000). The current number of clusters with S-Z determined distances is sufficiently large that a plot of d_A vs. redshift (a Hubble diagram) is now quite of interest, but with the present level of uncertainties the limits on the value of Ω are not very meaningful (as can be seen from figure 11 of Carlstrom $et\ al.$ 2000).

CMB anisotropy induced by the S-Z effect (Sunyaev 1977, Rephaeli 1981) is the main source of secondary anisotropy on angular scales of few arcminutes. Because of this, and the great interest in this range of angular scales – multipoles (in the representation of the CMB temperature in terms of spherical harmonics) $\ell \geq 1000$ – the S-Z anisotropy has been studied extensively in the last few years. The basic goal has been to map its predicted ℓ dependence in viable cosmological, large scale structure, and IC gas models. The strong motivation for this is the need to accurately calculate the power spectrum of the full anisotropy in order to make precise global parameter determinations from large stratospheric and satellite databases. In addition, mapping the S-Z anisotropy will yield direct information on the evolution of the cluster population.

Results from many calculations of the predicted S-Z anisotropy are not always consistent even for the same cosmological and large scale structure parameters. This is simply due to the fact that the calculation involves a large number of input parameters in addition to the global cosmological parameters ($e.g.,$ the present cluster density, and parameters characterizing the evolutionary history of IC gas), and the sensitive dependence of the anisotropy on some of these. The anisotropy

can also be predicted – presumably more directly – from simulations of the S-Z sky based largely on results from cluster X-ray surveys and the use of simple scaling relations (first implemented by Markevitch *et al.* 1992).

The anticipated observational capabilities, to be achieved with long duration balloon-borne experiments and satellites, of detailed mapping of the small angular scale anisotropy, have motivated many recent works. Colafrancesco *et al.* (1997), and Kitayma *et al.* (1998), have calculated the S-Z cluster number counts in an array of open and flat cosmological and dark matter models, and Seljak *et al.* (2000) have recently carried out hydrodynamical simulations in order to generate S-Z maps and power spectra. Cooray *et al.* (2000) have, in particular, concluded that the planned multi-frequency survey with the Planck satellite should be able to distinguish between the primary and S-Z anisotropies, and measure the latter with sufficient precision to determine its power spectrum and higher order correlations.

The main characteristics of the predicted power spectrum of the induced S-Z anisotropy are shown in Figure 3. Plotted are the angular power spectrum functions, $C_\ell(\ell + 1)/2\pi$, vs. the multipole, ℓ, for both the primary and S-Z induced anisotropies in the standard CDM model with $\Omega = 1$, based on the work of Sadeh and Rephaeli (2001). Their treatment is an extension of the approach adopted by Colafrancesco *et al.* (1997), who used the Press & Schechter formulation for the calculation of the cluster density as function of mass and redshift, and normalized it at the current epoch by the observed X-ray luminosity function (see also Colafrancesco *et al.* 1994). IC gas was assumed to evolve in a simple manner consistent with the results of the EMSS survey carried out with the Einstein satellite. The primary anisotropy was calculated using the CMBFAST code of Seljak & Zaldarriaga (1996). The solid line shows the primary anisotropy which dominates over the S-Z anisotropy for $\ell < 3000$. The S-Z power is largely due to the thermal effect; this rises with ℓ and is maximal around $\ell \sim 1000$. In this model, the S-Z power spectrum contributes a fraction of 5% (10%) to the primary anisotropy at $\ell \simeq 1860$ ($\ell \simeq 2360$). The relative magnitude of the S-Z power is higher in the Λ-dominated CDM model with $\Lambda = 0.8$; 5% and 10% contributions occur at $\ell \simeq 1520$ and $\ell \simeq 1840$, respectively. It can be concluded from this (and other studies) that the S-Z induced anisotropy has to be taken into account if the extraction of the cosmological parameters from an analysis of measurements of the CMB power spectrum at $\ell > 1300$ is to be precise.

5   Future Prospects

Work on the S-Z effect has greatly advanced in the last few years, and the prospects are very good for major improvements in the near future. The full potential of the effect as an important cosmological probe will be realized when high quality spectral and spatial mapping of the effect in *nearby* clusters, $z \leq 0.1$, will be feasible. The main limitation on the accuracy of the cosmological parameters will continue to be due to systematic uncertainties, which can be most optimally controlled when sensitive S-Z and X-ray measurements are made of nearby clusters. The interferometric CBI array extended the capability of the BIMA and OVRO arrays to obtain sensitive maps of the effect in nearby clusters. The currently operational XMM and
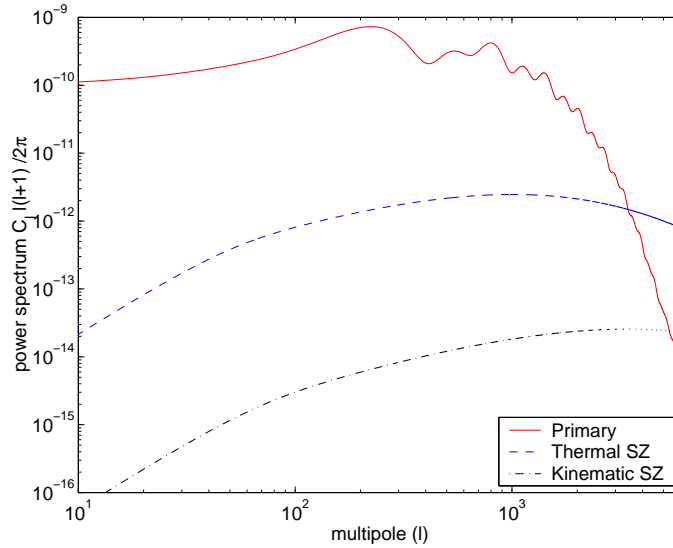
Figure 3. Primary and S-Z power spectra in the flat CDM model (Sadeh & Rephaeli 2001). The solid (red) line shows the primary anisotropy as calculated using the CMBFAST computer code of Seljak & Zaldarriaga (1996). The dashed (blue) line shows the thermal S-Z power spectrum, and the dotted-dashed (black) line is the contribution of the kinematic component.

Chandra satellites provide state-of-the-art X-ray spectral and spatial capabilities. Use of the S-Z spectrum as a powerful diagnostic tool will soon be possible when sensitive multi-frequency bolometric array experiments, with spectral bands in the range $150 - 350$ GHz, and very good spatial resolution ($\sim 3'$), become operational. Both ground-based (*e.g.,* the upgraded MITO experiment) and stratospheric (*e.g.,* BOOST, OLIMPO) projects are underway. Measurements of a large number of clusters with these and the currently operational arrays will enable a much more precise determination of the cosmological parameters. In particular, it will be possible to measure H_0 with an overall uncertainty of just $\sim 5\%$.

References

1. M. Birkinshaw, Phys. Rep. **310**, 97 (1999).
2. J.E. Carlstrom, M. Joy and L. Grego, ApJ **456**, L75 (1996).
3. J.E. Carlstrom *et al.*, Physica Scripta **60**, 1999 (.)
4. J.E. Carlstrom *et al.*, preprint 2000.
5. S. Colafrancesco, P. Mazzotta, Y. Rephaeli and N. Vittorio, ApJ **433**, 454 (1994).
6. S. Colafrancesco, P. Mazzotta, Y. Rephaeli and N. Vittorio, ApJ **479**, 1 (1997).
7. A. Challinor and A. Lasenby, ApJ **499**, 1 (1998).
8. L. Cooray, W. Hu and M. Tegmark, astro-ph/0002238.

9. F.X. Desert *et al.*, New Astron. **3**, 655 (1998).
10. D.M. Fabricant, M., Lecar and P. Gorenstein, ApJ **241**, 552 (1980).
11. L. Grego *et al.*, ApJ **in press**, 2001 (.)
12. W.L. Holzapfel *et al.*, ApJ **480**, 449 (1997a).
13. W.L. Holzapfel *et al.*, ApJ **481**, 35 (1997b).
14. J.P. Hughes and M. Birkinshaw, ApJ **501**, 1 (1998).
15. N. Itoh, Y. Kohyama and S. Nozawa, ApJ **502**, 7 (1998).
16. N. Itoh, S. Nozawa and Y. Kohyama, astro-ph/0005390.
17. M. Jones *et al.*, Nature **365**, 320 (1993).
18. T. Kitayama, S. Sasaki and Y. Suto PASJ **50**, 1 (1998).
19. A.S. Kompaneets, Soviet Phys.-JETP **4**, 730 (l957).
20. J.M. Lamarre *et al.*, ApJ **507**, L5 (1998).
21. M. Markevitch *et al.*, ApJ **395**, 326 (1992).
22. P.D. Mauskopf *et al.*, ApJ **538**, 505 (2000).
23. S. Nozawa, N. Itoh and Y. Kohyama, ApJ **507**, 530 (1998a).
24. S. Nozawa, N. Itoh and Y. Kohyama, ApJ **508**, 17 (1998b).
25. S. Nozawa, N. *et al.*, ApJ **536**, 31 (2000).
26. E. Pointecouteau *et al.*, ApJ **519**, L115 (1999).
27. Y. Rephaeli, ApJ **245**, 351 (1981).
28. Y. Rephaeli, ARA&A **33**, 541 (1995a).
29. Y. Rephaeli, ApJ **445**, 33 (1995b).
30. Y. Rephaeli and O. Lahav, ApJ **372**, 21 (1991).
31. Y. Rephaeli and D. Yankovitch, ApJ **481**, L55 (1997).
32. S. Sadeh and Y. Rephaeli, preprint (2001).
33. S.Y. Sazonov R.A. Sunyaev, ApJ **508**, 1 (1998).
34. S.Y. Sazonov R.A. Sunyaev, MN **310**, 765 (1999).
35. U. Seljak and M. Zaldarriaga, ApJ **469**, 437 (1996).
36. M. Shimon and Y. Rephaeli, preprint (2001).
37. R.A. Sunyaev, Comm. Ap.Sp.Phys. **7**, 1 (1977)
38. R.A. Sunyaev and Y.B. Zeldovich, Comm. Ap.Sp.Phys. **4**, 173 (1972).
39. R.A. Sunyaev and Y.B. Zeldovich, MN **190**, 413 (1980).
40. P.S. Udomprasert, B.S. Mason and A.C.S. Readhead, astro-ph/0012248.
41. Y.B. Zeldovich and R.A. Sunyaev, Ap.Sp.Sci. **4**, 301 (1969).